journal

J. Am. Ceram. Soc., **90** [2] 533–540 (2007)
DOI: 10.1111/j.1551-2916.2006.01410.x

Oxide Materials with Low Thermal Conductivity

Michael R. Winter and David R. Clarke[†]

Materials Department, College of Engineering, University of California, Santa Barbara, California 93160-5050

A heuristic approach to identifying candidate materials with low, temperature-independent thermal conductivity above room temperature is described. On the basis of this approach, a number of compounds with thermal conductivities lower than that of 8 mol% yttria-stabilized zirconia and fused silica have been found. Three compounds, in particular, the $Zr_3Y_4O_{12}$ delta phase, the tungsten bronzes, and the $La_2Mo_2O_9$ phase, exhibit potential for low thermal conductivity applications. As each can exhibit extensive substitutional solid solution with other, high atomic mass ions, there is the prospect that many more compounds with low thermal conductivity will be discovered.

I. Introduction

With some exceptions, the majority of non-metallic compounds exhibit a thermal conductivity that decreases with increasing temperature above room temperature.[1–4] Two notable exceptions are fused silica[2] and stabilized zirconia[4–6] (and the structurally related defect fluorite compounds ceria, thoria, and urania[3]). These two materials also have the lowest thermal conductivity of any fully dense oxide (Fig. 1).

One of the applications of yttria-stabilized zirconia (YSZ) that takes advantage of its unusually low thermal conductivity is as a thermal barrier coating for combustors and turbine blades in gas turbine engines, enabling them to operate at higher gas temperatures than without the coating. To further increase engine performance, there has been interest in finding an alternative material with still lower, temperature-independent thermal conductivity up to high temperatures. The discovery that certain rare-earth zirconates[4,7] with the pyrochlore crystal structure have lower thermal conductivity than YSZ and also exhibit an almost flat temperature dependence has demonstrated that stabilized zirconia is not unique among crystalline oxides in this respect and has spurred interest in the search for other oxides that also have low thermal conductivity. Although the pyrochlore zirconates have a crystal structure closely related to the basic fluorite structure of stabilized zirconia, the fact that their conductivity is lower than YSZ suggests that there is potential for many other materials with low thermal conductivity.

In this contribution, we describe some of the results of our search for oxide materials having low thermal conductivity. This paper is organized as follows: after a description of our approach to identifying candidate materials with low thermal conductivity and a brief description of experimental details, we present our results in sections devoted to different classes of material. For the purposes of this work, we include only those materials that proved to have thermal conductivities lower than that of dense YSZ. Although arbitrary, it serves to identify those materials that might, for instance, be of interest in future thermal barrier coating systems. Our focus has been on fully dense materials so that we can compare the intrinsic thermal conductivity of materials as it is well known that porosity can significantly decrease the measured thermal conductivity.

II. Criteria for Low Thermal Conductivity

Although no theory exists for predicting which compounds will have a low thermal conductivity at high temperatures, there are a number of guidelines that we have used to identify candidate materials. The first are expressions for what has become known as the minimum thermal conductivity, $\kappa_{\min}$.[8–10] This is the lowest thermal conductivity that a non-metallic solid can exhibit based on its atomic number density, its phonon spectrum, and other parameters.[8] Of particular interest to our work is the high-temperature limit to the minimum thermal conductivity, which is based on the assumption that the phonon mean free path approaches the mean inter-atomic distance. A number of similar expressions have been derived for this high-temperature limit.[8–10] For instance, Cahill and Pohl[9] have expressed this as

$$\kappa_{\min} = \frac{k_B}{2.48} n^{2/3}(2v_t + v_l) \qquad (1)$$

where n is the number of atoms per unit volume and v_t and v_l are the transverse and longitudinal sound velocities. An alternative expression, based on the same limiting conditions for the phonon mean free path and the effective atomic masses, that also gives almost the same values for simple compounds but is expressed in more easily obtained physical parameters is:[10,11]

$$\kappa_{\min} = 0.87 k_B \overline{\Omega}^{-2/3} (E/\rho)^{1/2} \qquad (2)$$

where $\overline{\Omega}_a$ is an effective atomic volume

$$\overline{\Omega}_a = \frac{M}{m\rho N_A} \qquad (3)$$

where M is the mean atomic mass of the ions in the unit cell, m is the number of ions in the unit cell, ρ is the density, and E is Young's modulus. k_B and N_A are Boltzmann's constant and Avagadro's number.

These expressions indicate that a large mean atomic mass and a low elastic modulus favor low thermal conductivity. Although helpful as a first step in selecting materials, one would not identify silica glass as having an especially low thermal conductivity on this basis nor do they provide any additional insight into the types of crystal structure that may exhibit low thermal conductivity.

To proceed, we have been guided by two additional concepts. One is to introduce randomly distributed point defects into a structure at a sufficiently high density that they will cause inelastic phonon scattering, thereby decreasing the phonon mean free path and decreasing the attainable thermal conductivity. There are a number of classic examples of this effect. These include the decrease in thermal conductivity of AlN with the concentration of oxygen impurities[12] and the increase in thermal conductivity of diamond when it is made of isotopically pure carbon.[13] Similarly, both the alloying of germanium with silicon[14] and the alloying of indium with GaAs[15] decrease the ther-

---

N. Padture—contributing editor

Manuscript No. 21956. Received June 29, 2006; approved October 4, 2006.
This work was supported by the Office of Naval Research as part of the TBC MURI grant through contract N014-02-1-0801.

[†]Author to whom correspondence should be addressed. e-mail: clarke@engineering.ucsb.edu

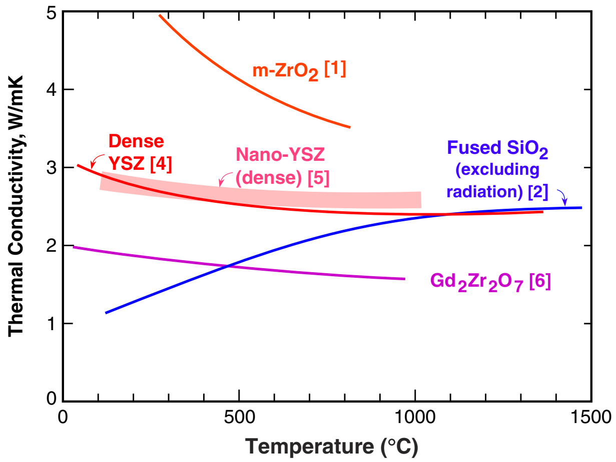

Fig. 1. Thermal conductivity of a number of oxide materials including monoclinic zirconia,[1] dense yttria-stabilized zirconia (YSZ),[4,6] the $Gd_2Zr_2O_7$ pyrochlore,[6] and, for comparison, fused silica.[2] There are several reports of the thermal conductivity of the pyrochlores but only Wu *et al.* [6] is for fully dense material.

mal conductivity of both these semiconductors. Kingery[1] also showed that solid solution alloying in the NiO–MgO system decreased the thermal conductivity. However, in each of these materials, as well as alloying in a variety of minerals[16] and mixed halides, cyanides, and fluorides,[17] the effect is to decrease the thermal conductivity in the $1/T$ regime of thermal conductivity. No effect has been reported in the high-temperature regime but there is no reason to suppose that alloying, or mass disorder, will also not be effective in the high-temperature regime. As we will show, this can, in fact, be quite effective in reducing thermal conductivity at high temperatures, especially when alloying is used to create disorder on more than one of the sub-lattices in a crystal structure.

The second concept is to seek structures that have the opposite characteristics of materials with very high thermal conductivity.[18] Such materials, for instance diamond, beryllium oxide, silicon carbide, aluminum nitride, and gallium nitride, have low atomic mass; highly directional, usually covalent, bonding; high lattice stiffness; high purity; low defect concentration; and minimum disorder in addition to being electrical insulators. These common characteristics lead to high phonon velocities and minimization of phonon scattering. Silica glasses are the classic example of materials that exemplify this set of opposite characteristics. Although silica glass has a low density and is primarily covalent, it has a flexible structure consisting of corner-shared SiO_4 tetrahedra that can rotate and flex about one another. The contrary behavior of silica glasses was attributed, as long ago as 1949 by Kittel,[19] to being a consequence of the amorphous structure precluding the existence of long wavelength phonons so that the phonon mean free path is limited by the size of the SiO_4 tetrahedral structure. Using the simple Debye model for thermal conductivity and using the measured thermal conductivity, first Kittel[19] and then Kingery[1] calculated that the phonon mean free path corresponds closely to the size of the tetrahedral unit. Although no non-silicate glass is known to be stable to high temperatures, it does suggest that crystal structures with various forms of short-range disorder and consisting of structural units that are loosely connected may also exhibit low thermal conductivity.

Taken together, these guiding concepts suggest that materials having low thermal conductivity at high temperature will be those that have high mean atomic mass, weak, non-directional bonding as well as extensive disorder at a variety of length scales down to that corresponding to inter-atomic spacings. Not all of these structures will be stable to the very highest temperatures required for thermal barrier application but may help identify other compounds with higher melting temperatures. This is an alternative to the search approach based on first identifying compounds that have the highest melting temperatures, such as appears to be the basis for a number of other searches.[7,20,21]

III. Experimental Procedure

Unless otherwise described, all the materials studied in this work were performed by what will be referred to as standard powder processing routes in which commercially available oxide powders were first mixed together, milled, ground, and then sintered to full density. Deviations from this method were necessary for compositions that did not densify easily and these are described where appropriate in the sections devoted to specific materials. In the standard process, the powders were mixed together and attrition milled for 3 h in deionized water with zirconia grinding media. The milled powder was passed through a <325 mesh sieve, dried, and ground to break up large agglomerates. Then, the powders were formed into disks by uniaxial cold pressing (80 MPa) without a binder and sintered in air, typically at 1600°C. Once dense samples were created, they were machined to size for thermal diffusivity measurements using a surface grinder. Some materials had to be hot pressed. These were also ground to size after removing any graphite that had adhered to the surfaces as well as any reaction zone. Finally, all the samples were annealed in air at 1000°C for 30 min to equilibrate them before testing. The density was measured using the Archimedes technique. The values are listed in Table I, together with the method used to make the samples.

X-ray diffraction analysis and Raman spectroscopy were used to confirm that the materials had the desired crystal structure and were single phase. The thermal conductivity, κ, of each of the materials was determined from separate measurements of the thermal diffusivity, α, heat capacity, C, and density, ρ, using

Table I. Sample Density and Processing

Compound	Measured density (kg/m^3)	X-ray density (kg/m^3)	Density (%)	Processing
7YSZ	6.04	6.134	98.5	Hot pressed/1600°C/60 min
$GdPO_4$	5.94	6.061	98.0	Hot pressed/1200°C/30 min
$LaPO_4$	4.60	5.067	90.8	Hot pressed/1150°C/45 min
YPO_4	3.63	4.262	85.2	Hot pressed/1550°C/60 min
$Gd_{0.5}La_{0.5}PO_4$	5.48	5.564	98.5	Hot pressed/1200°C/30 min
$Zr_3Y_4O_{12}$	5.45	5.49	99.3	Sintered in air/1600°C/2 h
$0.1WO_3$–$0.9Nb_2O_5$	4.70	4.74	99.2	Hot pressed/1275°C/30 min
$WNb_{12}O_{33}$	4.70	4.76	98.7	Hot pressed/1275°C/30 min
$W_4Nb_{26}O_{77}$	4.78	4.93	97.0	Hot pressed/1275°C/30 min
$W_3Nb_{14}O_{44}$	5.02	5.02	100	Hot pressed/1275°C/30 min
(3.5Eu–3.5Tm–7Y) SZ	6.25	6.24	100	Hot pressed/1550°C/60 min
(3.5Eu–3.5Yb–7Y) SZ	6.17	6.25	98.7	Hot pressed/1550°C/60 min
$La_2Mo_2O_9$	5.02	5.564	90.2	Sintered in air/1050°C/10 h

Table II. Atomic Mass and Ionic Radii (Ionic Radii after Shannon[43])

Ion	Zr^{4+}	Hf^{4+}	Y^{3+}	Tm^{3+}	Eu^{3+}	Yb^{3+}	La^{3+}	Gd^{3+}
Atomic mass (amu)	91.2	178.58	88.91	168.93	151.96	173.04	138.91	157.25
Ionic radius (nm)	0.084	0.083	0.1019	0.0994	0.1066	0.0985	0.1160	0.1053

the relationship

$$\kappa = \rho C_P k \tag{4}$$

Thermal diffusivity was measured with an Anter Flashline 3000 thermal flash system (Pittsburgh, PA) based on the technique pioneered by Parker *et al.*[22] This instrument uses a high-speed xenon lamp and measures the corresponding increase in backside temperature with an InSb infrared detector. All the samples were ground coplanar to a thickness of approximately 1 mm and a diameter of approximately 12.4 mm. To minimize radiative heat transport through the sample, which can lead to an apparently higher diffusivity, both sides were coated with a 10 nm Ti adhesion layer and a 750 nm of Pt layer via electron beam physical vapor deposition. Both sides were also spray coated with a colloidal graphite approximately 10 μm thick to ensure full absorption of the flash at the front surface and maximum emissivity from the backside. The samples were then heated to drive off any remaining solvents. The mass of the sample was measured before and after the test to ensure that the graphite coating remained intact. Thermal diffusivity was measured at 100°C intervals from 100° to 1000°C and then allowed to cool to 100°C before a final measurement was made. A comparison of the diffusivities measured at 100°C at the beginning and end of the test series was made to ensure that there were no changes in the sample or in the coating integrity. All the measurements were made in nitrogen. The thermal diffusivity was determined using the correction described by Clarke and Taylor,[23] which accounts for radiative losses that occur due to non-adiabatic conditions. Calibration of the thermal flash system was performed with a standard sample of pyroceram 9606 glass–ceramic. The pyroceram sample was purchased from Anter Corporation (Pittsburgh, PA). The day-to-day variation in the thermal diffusivity of the pyroceram sample was 2%–3%. Together with variations in the heat capacity measurements, the uncertainty in the reported values here of thermal conductivity is estimated to be ±5%.

Heat capacity was measured with a Netzsch Pegasus 404C differential scanning calorimeter (Estes, CO). Samples were ground coplanar to approximately 1 mm thickness and approximately 5.5 mm diameter. Heat capacity was determined according to the ASTM standard E1269-95 in a platinum crucible from room temperature to 1000°C in an argon atmosphere.[24]

IV. Decreasing Thermal Conductivity of Zirconia by Substitution on the Cation Sub-Lattice

YSZ has several of the characteristics of low conductivity described in Section II. Without stabilization by yttria (or another stabilizer ion, such as the trivalent rare-earth ion, divalent cations, or mixed-valence ions), zirconia is monoclinic and exhibits the classic $1/T$ temperature dependence.[1] The substitution of Y^{3+} for Zr^{4+} in the fluorite structure of ZrO_2 stabilizes the tetragonal phase by introducing vacancies into the oxygen sub-lattice. At typical concentrations of 8 *m*/*o* $YO_{1.5}$, the spacing of the oxygen vacancies is ~1.25 nm. (At higher yttria concentrations, the concentration of vacancies increases but clustering begins to occur.) The unusually low thermal conductivity of YSZ is generally attributed to enhanced phonon scattering from oxygen vacancies. Although the Y^{3+} ions substitute for Zr^{4+} ions in the cation sub-lattice, their atomic mass is almost identical to that of the Zr^{4+} ions and hence are unlikely to cause any mass disorder on the cation sub-lattice.

In a very important practical development, Zhu and Miller[25,26] at NASA Glenn have demonstrated that coatings stabilized with a combination of trivalent ions have exceptionally low thermal conductivity. These coatings have been referred to as "cluster-doped" coatings and are based on the substitution of three different trivalent cations, typically Y^{3+} ion plus one ion larger and one smaller. Unlike other coating materials, the thermal conductivity of these coatings did not change substantially over extended periods of time at high temperatures.[27]

An alternative approach to reducing thermal conductivity is to replace some of the Zr^{4+} ions with Hf^{4+} ions. In contrast to the rare-earth substitutions used in the "cluster"-doped zirconia, Hf^{4+} ions do not introduce vacancies into the oxygen sub-lattice but produce random mass disorder into the cation sub-lattice. A peculiar feature of Hf^{4+} ions is that they are chemically similar to Zr^{4+} ions, have a similar ionic radius but are almost twice as massive.

(1) Multiple Dopant Substitution

To evaluate the possible effect of multiple stabilizer dopants in fully dense material as distinct from coatings, we produced two sets of dense zirconia material stabilized with three different trivalent ions, Y^{3+} and Eu^{3+}, and either Yb^{3+} or Tm^{3+}. The ionic radii are listed in Table II. The total concentration of the stabilizer ions was 14 *m*/*o*, so that the material was tetragonal, an expectation confirmed by X-ray diffraction and Raman spectroscopy. The stabilizer concentration was chosen as the work of Zhu and Miller[25] indicates that coatings made with this total stabilizer concentration had the lowest thermal conductivity in their thermal gradient testing. The powders of these materials were prepared in the standard way but were then densified by hot pressing at 20 MPa for 1 h at 1550°C as they could not be densified by sintering. Even after sintering for 2 h at 1600°C, they only attained a density of ~70%.

The thermal conductivity of two of the fully dense materials is shown in Fig. 2. One, the composition stabilized with $7YO_{1.5}+3.5\ EuO_{1.5}$ and $3.5\ TmO_{1.5}$, had a temperature-independent conductivity of ~2.0 W/mK, independent of temperature. This value is almost the same as has been reported for zirconia stabilized with 14 *m*/*o* $YO_{1.5}$ [28] but much higher than that reported for the NASA coatings. The other, the one stabilized with $7YO_{1.5}+3.5\ EuO_{1.5}$ and $3.5\ YbO_{1.5}$, exhibited very

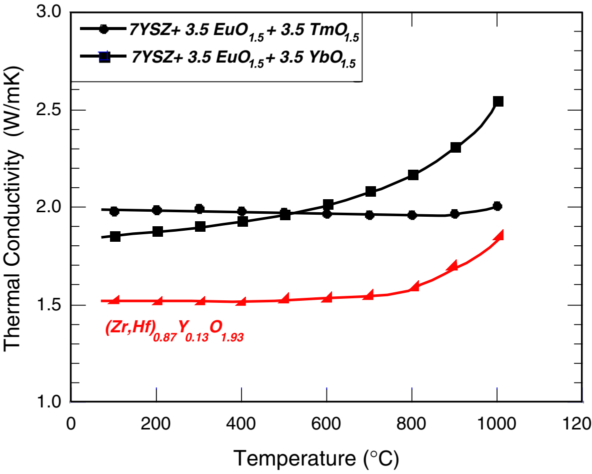

Fig. 2. Comparison of the thermal conductivity of two tri-doped zirconias and the equi-molar hafnia-zirconia material.

pronounced radiative transport effects from almost 300°C onwards. Why radiative effects are so pronounced in this composition is not known but was duplicated with a second sample. All the samples were white indicating extensive internal optical scattering. Nevertheless, at 100°C, the thermal conductivity was somewhat lower at ~1.8 W/mK. Two conclusions can be drawn from these results. The first is that it is the mean value of the ionic mass of the stabilizer ions that is important rather than the variation in ionic mass or size. The second, and of crucial importance for the design of coatings, is that the low thermal conductivity of the "cluster"-doped coatings is not intrinsic to the composition per se but most probably due to the presence of porosity incorporated during the deposition of the coating and its resistance to densification during deposition and subsequent high-temperature exposure.

(2) Hafnia Substitution

As described in detail elsewhere, hafnia substitution decreases the thermal conductivity of YSZ across the full solid–solution series.[29] The most notable reduction, however, occurs close to the equi-molar mixtures of hafnia and zirconia, such as $(Zr_{0.5}Hf_{0.5})_{0.87}Y_{0.13}O_{1.94}$ tetragonal and the $(Zr_{0.4}Hf_{0.6})_{0.76}Y_{0.24}O_{1.88}$ cubic phase. The data for the former composition are shown in Fig. 2 and, for comparison, with the thermal conductivity of the multiple-stabilizer zirconia, illustrates the effectiveness of mass disorder on the cation sub-lattice. In contrast to the cluster-doped materials, these could be readily densified to better than 96% by sintering in air at 1600°C for 2 h. The measured lattice parameters and molecular weight were used to calculate the X-ray density of the individual compositions.

V. Thermal Conductivity of the Delta Phase $Zr_3Y_4O_{12}$

Previous studies have shown that the thermal conductivity of zirconia decreases with increasing yttria concentration up to about 20 *m*/*o* $YO_{1.5}$ but then is approximately constant.[28] This saturation behavior has been attributed to ordering of the substitutional Y^{3+} ions and the oxygen vacancies, limiting the random disordering on the oxygen sub-lattice.[30,31] The maximum concentration that seems to have been studied is 30% Y_2O_3, well within the cubic, fluorite phase. However, the ZrO_2–$YO_{1.5}$ phase diagram indicates that another crystalline phase, the delta phase, $Zr_3Y_4O_{12}$, exists.[32]

The experiment indicates that this compound does have a low and temperature-independent thermal conductivity as shown by the data in Fig. 3. Its thermal conductivity parallels the thermal conductivity of YSZ but has a value almost 30% lower up to at least 1000°C. The delta-phase composition was readily sintered in air at 1550°C for 2 h but could not be fully ordered even after 3 weeks at 1250°C.

(1) Hafnia Substitution in the Delta Phase

Based on the success in lowering the thermal conductivity by substituting Zr^{4+} ions with Hf^{4+} ions,[29] the equi-molar composition $(Zr_{0.5}Hf_{0.5})_3Y_4O_{12}$ was prepared in a fully dense form. Its thermal conductivity as a function of temperature is shown in Fig. 3 and demonstrates clearly that introducing mass disorder into the cation sub-lattice can significantly reduce thermal conductivity from room temperature up to at least 1000°C.

VI. Tungsten Niobates

In contrast to the zirconia-based oxides, the basis for selecting the tungsten niobates, sometimes referred to as the "tungsten bronzes," for study is that their crystal structures have some features common to silica. They consist of blocks of corner-shared NbO octahedra linked together with W ions.[33,34] This is illustrated for the $W_3Nb_{14}O_{44}$ compound in Fig. 4 showing the blocks of 4 × 4 corner-sharing octahedra joined by W ions and arranged in a tetragonal structure. According to the first crystal structure determination, the W and Nb ions were randomly distributed among all the octahedral sites. Further structural refinement by neutron diffraction indicates that, at room temperature at least, there is a preference for the W to be in an octahedral co-ordination and to be distributed among the octahedra in the vicinity of the block-sharing W ions. In selecting these compounds for study, it was also hypothesized that the corner sharing of the blocks and the disorder along the *c*-axis associated with the W ions might provide the vibrational freedom that would lead to low thermal conductivity. In addition, several of the tungsten bronzes have some of the highest mean atomic masses and densities of the oxides and several are stable to well over 1400°C. Also, the size of the blocks varies with the W/Nb ratio, leading to a series of line compounds in the phase diagram, as shown in Fig. 4.

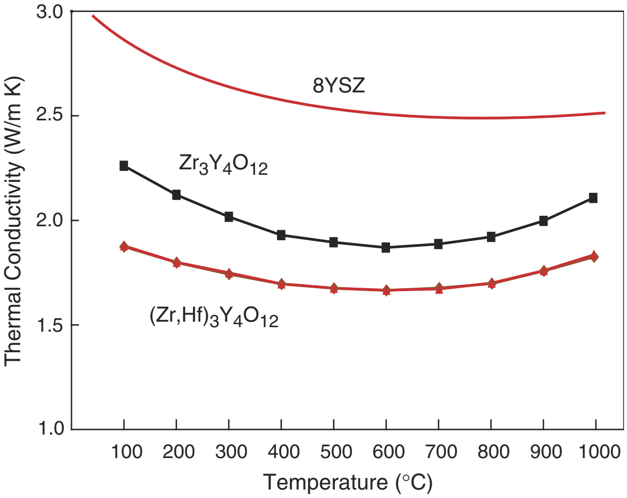

Fig. 3. Comparison of the thermal conductivity of the $Zr_3Y_4O_{12}$ delta phase and the hafnia–zirconia counterpart with that of dense yttria-stabilized zirconia (8YSZ).

Four compounds were investigated and are indicated in the diagram of Fig. 4. Three were single-phase line compounds having different W/Nb ratios, $W_3Nb_{14}O_{44}$, (D), $WNb_{12}O_{33}$ (B), and $W_4Nb_{26}O_{77}$ (C). The fourth was a deliberately made two phase mixture of $Nb_{12}WO_{39}$ and $Nb_{60}WO_{183}$ marked A on Fig. 4. All the compounds were made from oxides and were calcined at 1100°C for 2 h in air. They then had to be hot pressed and then annealed in air at 1000°C for 1 h.

The measured thermal conductivity (Fig. 5) indicates that the tungsten bronzes do indeed have low thermal conductivity and are temperature independent. The actual values are similar to those of both YSZ and fused silica. Notably, both the single-phase materials and the two-phase material exhibited similar conductivities.

VII. Lanthanide Orthophosphates

Orthophosphates have crystal structures that are analogous to the network silicates with various arrangements of corner- and edge-sharing PO_4 tetrahedra rather than the SiO_4 tetrahedra.[35] Based on the guidelines described in 'Section II,' they are a natural choice of compounds for searching for low thermal conductivity. Perhaps the best known example is the aluminum phosphate ($AlPO_4$) but an extensive series of lanthanide-based orthophosphates ($LnPO_4$), also exist, which have a significantly higher density because of the higher atomic mass of the lanthanide ion. They form two distinct, but closely related, crystal structures, the monazite and the xenotime structures, depending on the ionic size of the lanthanide ions.[36] The monazite structure is typically formed with the larger lanthanide ions and the xenotime structure with the smaller lanthanide ions. Both structures

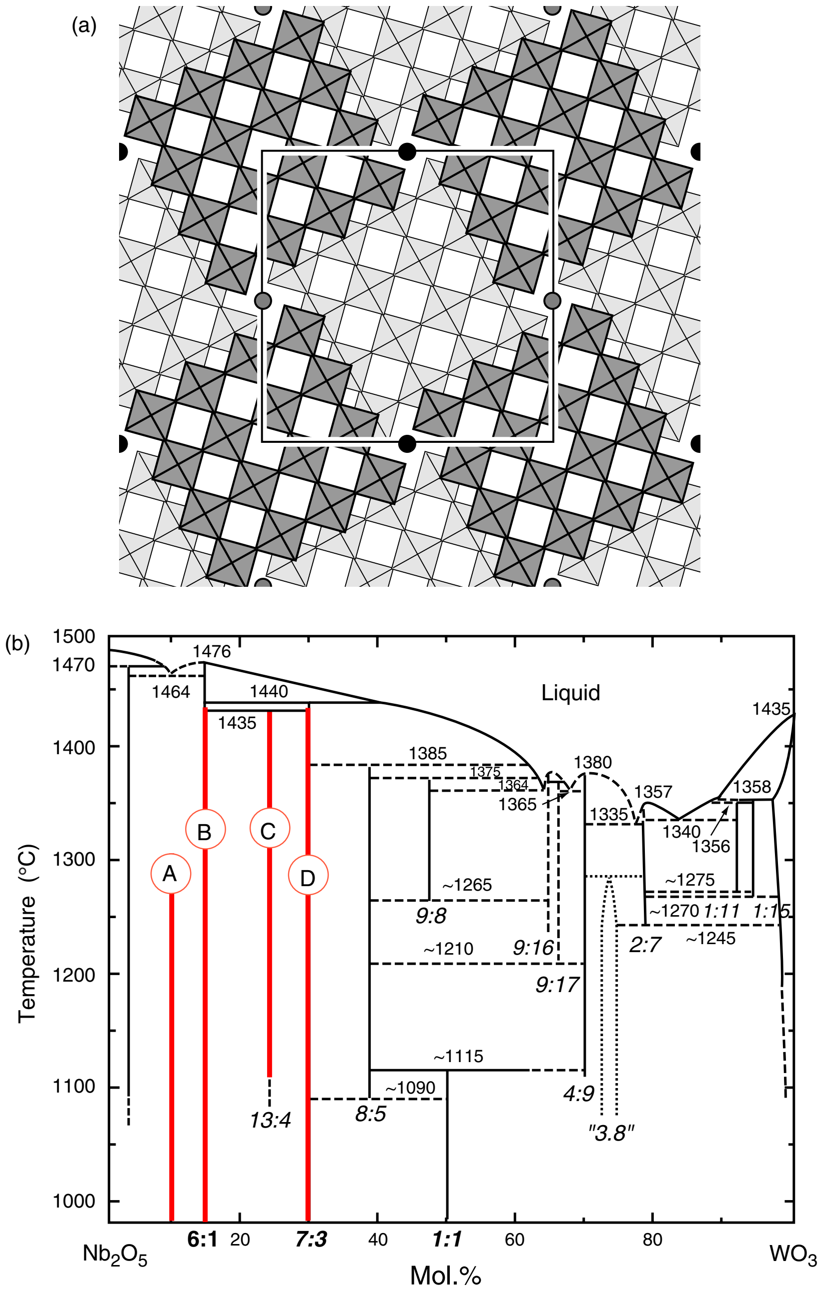

Fig. 4. (a) Schematic of the crystal structure of $W3Nb_{14}O_{44}$ looking down the tetragonal axis. The structure consists of blocks of 4 × 4 corner-sharing NbO octahedra joined by the tungsten ions shown as circles in the square unit cell. (b) Section of the Nb_2O_3–WO_3 phase diagram illustrating the compositions of the compounds, A, B. C and D measured.

are based on chains of alternating phosphate tetrahedral and RE polyhedra. Because of the well-known lanathanide ion contraction, these compounds are formed with the lighter and heavier ions, respectively. The boundary between the monazite and xenotime structures occurs between the $GdPO_4$ and the $TbPO_4$ compounds, the monazite being formed with the Gd^{3+} ions and the xenotime being formed with the Tb^{3+} ions.

It has been reported that the monazite compound $CePO_4$ has a thermal conductivity of ~3.1 W/mK at room temperature and a value of ~1.8 W/mK at 500°C[37], suggesting a weak $1/T$ dependence. Similarly, the xenotime compounds YPO_4, $LuPO_4$, $YbPO_4$, and $ErPO_4$ all have a thermal conductivity of ~12 W/mK at room temperature.[38] The thermal conductivity of $LaPO_4$ at room temperature has previously been reported.[39]

To compare the thermal conductivity of a number of the monazite and xenotime structures, we measured the conductivity of YPO_4 (a xenotime compound) and $GdPO_4$ and $LaPO_4$, both having the monazite structure. We also investigated the co-doped $(La_{0.5}Gd_{0.5})PO_4$, another monazite compound. The rationale for the last was that although it has a different crystal structure, it has the same unit cell volume as does YPO_4 and so one might expect that the average inter-atomic spacing would be the same. The materials were made from chemically precipitated precursor powders prepared by adding phosphoric acid, drop by drop, to the appropriate nitrate solution in deionized water. The powders were washed several times with deionized water and centrifuged between washings to avoid powder loss. Then, they were calcined at 700°C for 1 h in air. Before hot pressing, the powders were heated above 500°C to remove any water as they are hygroscopic. The YPO_4 was hot pressed at 1550°C, whereas the monazite compounds were hot pressed at 1200°C. Even under these conditions, not all the materials were fully dense; the YPO_4 samples were ~85% dense and the $LaPO_4$ samples were 90% dense. Both the $GdPO_4$ and $(La_{0.5}Gd_{0.5})PO_4$ samples were 98% dense. Two samples of each composition were made.

The measured thermal conductivities are shown in Fig. 6. The most striking feature of the data is that the orthophosphate with

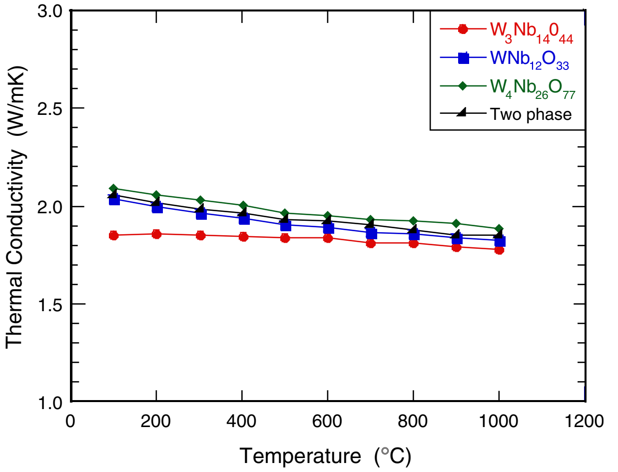

Fig. 5. Measured thermal conductivity of the tungsten–bronzes indicated.

the xenotime structure has the classic $1/T$ dependence, whereas the three with the monazite structure are almost independent of temperature. Furthermore, the co-doped monazite, $(La_{0.5}Gd_{0.5})PO_4$, clearly has quite different conductivity characteristics from the xenotime YPO_4 even though the average inter-atomic distance is the same. Although the atomic mass of the cations is rather similar, the difference in temperature dependence appears to be directly related to the difference in the way in which the basic building blocks are connected. We also note that although the three monazites have different unit cell volumes, they have rather similar thermal conductivities. The most obvious difference between the xenotime and monazite structures is that the xenotime structure, which has a higher crystal symmetry, consists of REO_8 polyhedra whereas the polyhedra in the monazites are REO_9.[36] This would suggest that the bonds are weaker in the monazite than in the xenotime structures. The other distinct difference is that there is much greater variation in the RE–O bond length in the monazite, with each of the nine bonds being different than in the xenotime structure where there are only RE–O bond lengths.[36] Similarly, the RE–P bond length in the xenotime is shorter than either of the two RE–P bond lengths in the monazites. In addition, in looking along the [001] axis, it is evident that there is some rotation of the PO_4 tetrahedra about the [001] direction in the monazite, whereas the tetrahedra are all parallel in the xenotime structure. Finally, in the monazite structure, the PO_4 tetrahedra are linked to the REO_9 polyhedra by corner sharing, whereas in the xenotime structure, some of the tetrahedra are linked to the REO_8 polyhedra by corner sharing and others are edge shared. All these facts suggest that the monazite structure is more disordered at the inter-atomic length scale than the xenotime structure, consistent with the significantly lower thermal conductivity.

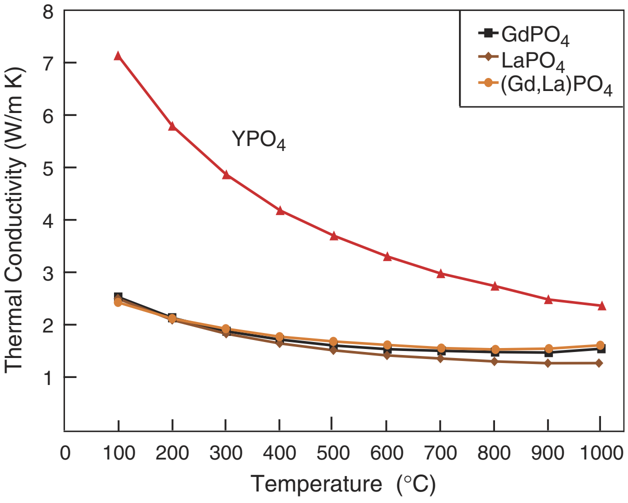

Fig. 6. Comparison of the thermal conductivity of the xenotime-structured YPO_4 and three of the monazite compounds. The YPO_4 material tested was 85% dense and the monazites were all 90% of full density.

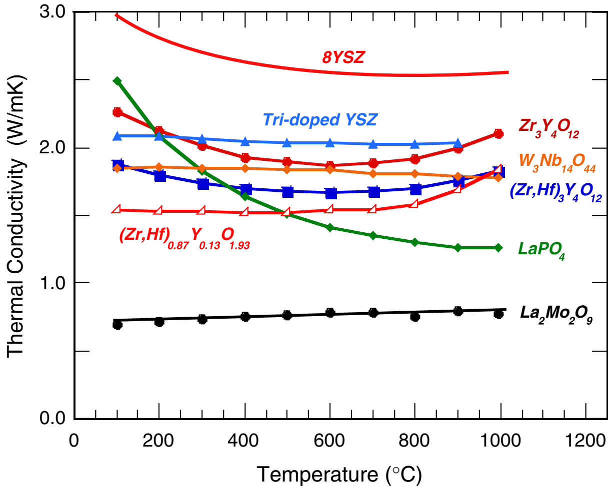

Fig. 7. Thermal conductivity of $La_2Mo_2O_9$ compared with the other materials investigated in this work. The density of the $La_2Mo_2O_9$ samples was 90%.

A more extensive survey of the orthophosphates is clearly warranted but we had difficulty in making large enough, fully dense pellets for thermal diffusivity measurements to explore other ionic substitutions.

VIII. Lanthanum Molybdate

Lanthanum molybdate, $La_2Mo_2O_9$, is a recently discovered compound that has attracted considerable attention because it exhibits a two to three order of magnitude increase in ionic conductivity to a value comparable with that of YSZ, when the crystal structure changes on heating at ~585°C.[40] Our original motivation for studying the thermal conductivity of this compound was simply to ascertain whether the change in crystal structure would affect the thermal conductivity, the rationale being that a compound with a very high oxygen ionic conductivity would have considerable vibrational entropy of the oxygen sub-lattice and this might be reflected by strong phonon scattering and hence low thermal conductivity. However, as our measurements show in Fig. 7, there was no discernable change in thermal conductivity as the crystal structure changed and almost no variation with temperature. The samples were made by attrition milling of the oxides for 3 h in deionized water, followed by grinding and then calcination in air for 16 h at 800°C. They were then cold pressed and sintered in air at 1000°C for 48 h. They could not be prepared by hot pressing, presumably because of the reaction to form molybdenum carbides. Four samples were made on separate occasions. Each had a density of ~90% and all showed almost identical thermal conductivity. Using Maxwell's relation[1,41] to account for the porosity, ϕ,

$$\kappa_{\mathrm{dense}} = \kappa_{\mathrm{measured}} \frac{1}{(1 - 1.5\phi)} \tag{5}$$

the thermal conductivity of dense lanthanum molybdate would be 17% higher than shown in Fig. 7, namely 0.82 W/mK at 100°C and 0.95 W/mK at 1000°C.

Remarkably, our results show that the thermal conductivity is lower than that of any other crystalline compound we have measured or found in the literature. Part of the reason for its low thermal conductivity is undoubtedly its large mean atomic mass.

However, this alone does not explain its exceptionally low conductivity. It is noted, though, that in common with the zirconate pyrochlores, it also has a high concentration of "structural vacancies."

IX. Discussion and Conclusions

As mentioned in Section I, it was once considered that YSZ was exceptional for a crystalline material because it exhibits both a low thermal conductivity at room temperatures and a conductivity that is constant to high temperatures. However, as the results presented here indicate, several compounds with lower thermal conductivity than YSZ have been identified. While the approach we have used to identify these compounds is, by its very nature, qualitative it does suggest that there will be many other compounds that will also have a lower thermal conductivity than YSZ.

On the basis of the materials identified, three strategies appear to be most promising in identifying low thermal conductivity materials. One is to search for silicate-like structures with a large effective mass that incorporate structural units that are joined together by rather flexible linkages. A second is to seek out compounds with low crystal symmetry. The third is to introduce mass disorder on the cation sub-lattices of a crystal structure that is known to have rather low thermal conductivity. The concept of introducing mass disorder to lower thermal conductivity is not, of course, new. However, hitherto it has only been shown to be effective in the temperature regime where the thermal conductivity is dependent on temperature, the $1/T$ regime. This work demonstrates that the mass disorder strategy is also a viable one in the minimum thermal conductivity regime, the regime where the thermal conductivity is temperature independent.

At this stage, very little is known about the phase equilibria of the $La_2Mo_2O_9$ and related compounds to ascertain whether they might have applications as thermal insulators or in other applications beyond fast-ion conductors. It is also unknown how their melting temperatures vary with the rare-earth ion substitution for the lanthanum ion. Similarly, although the orthophosphates have attractively low thermal conductivity, controlling their stoichiometry during deposition has proven problematic and any free phosphate is likely to corrode existing superalloys. Of the compounds investigated in the course of our studies, the zirconia–yttria delta phase therefore appears to be the most promising for possible application in thermal barrier coatings. The delta phase is reported to be stable to $\sim$1346°C before transforming to cubic zirconia and the composition itself does not melt until 2461°C. In addition, the constituent elements are known to have similar vapor pressures and hence it is likely that the compound can be deposited by standard, one-source electron beam deposition. As it is not phase compatible with alumina, the oxide formed by high-temperature oxidation of the majority of bond-coat alloys, it would need to be used in a two-layer configuration with standard 8YSZ as an inner layer providing the thermal cycle resistance. Finally, it is noted that the zirconia–yttria delta phase is just one of a family of compounds with the same crystal structure and that cation substitution can be made on both the Zr site and on the Y site, so there a possibility of systematically varying the cations to investigate the effect on thermal conductivity as has been done for the pyrochlore compounds through modeling.[42]

It is interesting to speculate as to why the pyrochlore zirconates, the delta phase, the tungsten bronzes, and the lanthanum molybdate all exhibit such low thermal conductivity. One common characteristic is that they have more than one cation sub-lattice and hence the possibility of different phonon modes as well as disorder on each. They all have a large average atomic volume, Ω, as shown in Table III and calculated from published data on densities and formula units per unit cell. Another common characteristic of the unit cells of these compounds is that they all incorporate "structural vacancies." These oxygen vacancies can be expected to limit the allowable lattice phonons as well as produce phonon scattering when they are occupied. However, as they are not randomly distributed, by analogy with the oxygen vacancy ordering in YSZ at high yttria concentrations, it is unlikely that they can be more effective in phonon scattering than they are in that material. Several of the compounds also appear to have unusually large thermal ellipsoids for the oxygen ions as measured by X-ray diffraction at room temperature, suggesting that they may be particularly effective in phonon scattering. Another characteristic, though, of the oxygen sub-lattice in the delta phase as well as both the cation and anions sub-lattices in the pyrochlore compounds is that they have a Kagome arrangement.[44] This is an unusual feature for the anion sub-lattice in solids but is likely to support unusual phonon modes.

Table III. Calculated Average Atomic Volume

Compound	Average atomic volume Ω (nm^3)
7YSZ	0.1158
YPO_4	0.1194
$LaPO_4$	0.1278
$Zr_3Y_4O_{12}$	0.1308
$Gd_2Zr_2O_7$	0.1330
$W_3Nb_{14}O_{44}$	0.1385
$La_2Mo_2O_9$	0.1410

One of the correlations that we have noted is that all these compounds have rather broad Raman lines, and in some cases, rather poorly defined Raman spectra. An example is shown in Fig. 8. Although we are not aware of any direct correlation between thermal conductivity and the width of the Raman lines, the phonon lifetime, τ, is inversely proportional to the FWHM of the Raman lines when the lines are not instrumentally limited.[45] As the phonon mean free path can be expected to be proportional to the phonon lifetime, then if the mean phonon velocity remains unchanged, there will be a correlation between the thermal conductivity and the width of the Raman lines.

Lastly, it is appropriate to mention that although all the samples were the same thickness and were either white or dark colored before metal coating, some nevertheless showed appreciable "transparency" in the thermal diffusivity measurements even at relatively low temperatures. Interestingly, increasing the thickness of the platinum layer to 2.25 μm on both sides did not affect the observation. Also, as indicated in Fig. 2, there could be a significant difference with only a minor change in the stabilizer ion. The transparency is not the penetration of the flash of light through the absorbing layer and the sample that is

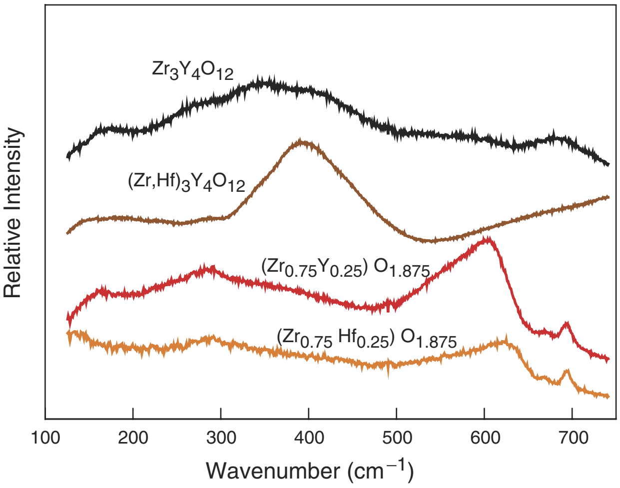

Fig. 8. Raman spectra of the indicated compounds recorded with a 514 nm argon ion laser. The spectra are characterized by broad Raman bands much broader than that of most oxides.

usually considered in papers on measuring diffusivity by the flash technique. As the center wavelength of the xenon flash is at $\sim$1.8 μm, it is unlikely that any light penetrates as it is a wavelength to which the carbon over coat is strongly absorbing and the platinum layer is highly reflective. Instead, it appears to be associated with radiation from the heated side through the sample to the other side that the detector senses. As the majority of the zirconia samples are intrinsically transparent into the mid-infra-red, despite the presence of optical scattering, the radiative contribution may be especially sensitive to the arrangement of pores in the samples that are close to being fully dense and hence containing a relatively few number of pores. Under such circumstances, there can be direct radiative paths through regions of the sample between pores. This effect is likely to be dependent on the thickness of the samples tested, being particularly pronounced for thin samples.

X. Summary

Heuristic arguments have been used to identify possible materials with low thermal conductivity at high temperatures. These arguments suggest that candidate materials can be identified by searching for compounds with a combination of high atomic mass, flexible ionic structures, non-directional bonding, and extensive site disorder. We also find that substitutional alloying on the cation sub-lattices is a viable approach to reducing thermal conductivity in the $\kappa_{\min}$ regime. Materials that exhibit low thermal conductivity generally also exhibit Raman spectra with very broad peaks. It is also concluded that compounds with low crystal symmetry and with a Kagome arrangement of ions might also exhibit unusually low thermal conductivity.

Acknowledgments

The authors are grateful to Dr. Kurt Sickafus of Los Alamos National Laboratory for discussions on pyrochlore and delta phases and for providing an unpublished copy of his work on characterizing crystal structures in terms of layers of cations and anions.

References

[1] W. D. Kingery, *Introduction to Ceramics, 2nd Edition*. Wiley Interscience, New York, 1976.

[2] K. L. Wray and T. J. Connolly, "Thermal Conductivity of Clear Fused Silica at High Temperatures," *J. Appl. Phys*., **30** [11] 1702–6 (1959).

[3] W. D. Kingery, "Thermal Conductivity: XII. Temperature Dependence of Conductivity for Single Phase Ceramics," *J. Am. Ceram. Soc*., **38** [7] 251 (1955).

[4] M. J. Maloney, "Thermal Barrier Coatings Systems and Materials"; U.S. Patent 6117560 (2000) filed 1996.

[5] S. Raghavan, H. Wang, R. B. Dinwiddie, W. D. Porter, and M. J. Mayo, "The Effect of Grain Size, Porosity and Yttria Content on the Thermal Conductivity of Nanocrystalline Zirconia," *Scr. Mater*., **39** [8] 1119–25 (1998).

[6] J. Wu, X. Wei, N. P. Padture, P. G. Klemens, M. Gell, E. Garcia, P. Miranzo, and M. I. Osendi, "Low Thermal Conductivity Rare-Earth Zirconates for Potential Thermal Barrier Coating Applications," *J. Am. Ceram. Soc*., **85** [12] 3031–5 (2002).

[7] R. Vassen, X. Cao, F. Tietz, D. Basu, and D. Stover, "Zirconates as New Materials for Thermal Barrier Coatings," *J. Am. Ceram. Soc*., **83** [7] 2023–8 (2000).

[8] G. A. Slack, "The Thermal Conductivity of Nonmetallic Crystals"; pp. 1–71 in *Solid State Physics*, **Vol 34**, Edited by F. Seitz and D. Turnbull, Academic Press, London, 1979.

[9] D. G. Cahill and R. O. Pohl, "Lattice Vibrations and Heat Transport in Crystals and Glasses," *Annu. Rev. Phys. Chem*., **39**, 93–121 (1988).

[10] D. R. Clarke, "Materials Selection Guidelines for Low Thermal Conductivity Thermal Barrier Coatings," *Surf. Coat. Technol*., **163–164**, 67–74 (2003).

[11] C. G. Levi, "Emerging Materials and Processes for Thermal Barrier Systems," *Curr. Opin. Solid State Mater. Sci*., **8**, 77–91 (2004).

[12] G. A. Slack, R. A. Tanzilli, R. O. Pohl, and J. W. Vandersande, "The Intrinsic Thermal Conductivity of AlN," *J. Phys. Chem. Solids*, **48** [7] 641–7 (1987).

[13] L. Wei, P. K. Kuo, R. L. Thomas, T. R. Anthony, and W. F. Banholzer, "Thermal Conductivity of Isotopically Modified Single Crystal Diamond," *Phys. Rev. Lett*., **70**, 3762–7 (1993).

[14] B. Abeles, D. S. Beers, G. D. Cody, and J. P. Dismukes, "Thermal Conductivity of Ge-Si Alloys at High Temperatures," *Phys. Rev*., **125**, 44 (1962).

[15] M. S. Abrahams, R. Braunstein, and F. D. Rosi, "Thermal, Electrical and Optical Properties of (In,Ga)As Alloys," *J. Phys. Chem. Solids*, **10**, 204–10 (1959).

[16] F. Birch and H. Clark, "The Thermal Conductivity of Rocks and Its Dependence Upon Temperature and Composition," *Am. J. Sci*., **238**, 529–58, 613 (1940).

[17] D. G. Cahill, S. K. Watson, and R. O. Pohl, "Lower Limit to the Thermal Conductivity of Disordered Crystals," *Phys. Rev*., **46** [10] 6131–40 (1992).

[18] G. A. Slack, "Nonmetallic Crystals with High Thermal Conductivity," *J. Phys. Chem. Solids*, **34**, 321–35 (1973).

[19] C. Kittel, "Interpretation of the Thermal Conductivity of Glasses," *Phys. Rev*., **75**, 972 (1949).

[20] X. Q. Cao, R. Vassen, and D. Stoever, "Ceramic Materials for Thermal Barrier Coatings," *J. Eur. Ceram. Soc*., **24**, 1–10 (2004).

[21] R. Vassen, F. Tietz, G. Kerkhoff, and D. Stoever, "New Materials for Advanced Thermal Barrier Coatings"; pp. 1627–35 in *Proceedings of the 6th Liege Conference. Materials for Advanced Power Engineering*, Edited by J. Lecomte-Beckers. Forschungszentrum Jülich, Jülich, Germany, 1998.

[22] W. J. Parker, R. J. Jenkins, C. P. Butler, and G. L. Abbott, "Flash Method of Determining Thermal Diffusivity, Heat Capacity and Thermal Conductivity," *J. Appl. Phys*., **32** [9] 1679–84 (1961).

[23] L. I. Clarke and R. Taylor, "Radiation Loss in the Thermal Flash Method for Thermal Diffusivity," *J. Appl. Phys*., **46** [2] 714–9 (1975).

[24] ASTM E1269-95. *Standard Test Method for Determining Specific Heat Capacity by Differential Scanning Calorimetry*. ASTM International, West Conshohocken, PA.

[25] D. M. Zhu and R. A. Miller, "Low Conductivity and Sintering Resistant Thermal Barrier Coatings"; U.S. Patent 7001859 B2, 2006.

[26] D. M. Zhu and R. A. Miller, "Thermal Conductivity and Sintering Behavior of Advanced Thermal Barrier Coatings," *Ceram. Eng. Sci. Proc*., **23**, 457–68 (2002).

[27] D. M. Zhu, Y. L. Chen, and R. A. Miller, "Defect Clustering and Nanophase Structure Characterization of Multi-Component Rare Earth Doped Zirconia–Yttria Thermal barrier Coatings," *Ceram. Eng. Sci. Proc*., **24**, 525–34 (2003).

[28] J-F. Bisson, D. Fournier, M. Poulain, O. Lavigne, and R. Mevrel, "Thermal Conductivity of Yttria–Zirconia Single Crystals, Determined with Spatially Resolved Infrared Thermography," *J. Am. Ceram. Soc*., **83** [8] 1993–8 (2000).

[29] M. R. Winter and D. R. Clarke, "The Thermal Conductivity of Yttria-Stabilized Zirconia–Hafnia Solid Solutions," *Acta Mater*., **54**, 5051–9 (2006).

[30] J. P. Goff, W. Hayes, S. Hull, M. T. Hutchings, and K. N. Clausen, "Defect Structure of Yttria-Stabilized Zirconia and Its Influence on the Ionic Conductivity at Elevated Temperatures," *Phys. Rev*., **B59** [22] 14202–19 (1999).

[31] T. R. Welberry and B. D. Butler, "Diffuse X-Ray Scattering from Disordered Crystals," *Chem. Rev*., **95**, 2369–403 (1995).

[32] H. G. Scott, "The Yttria–Zirconia Delta Phase," *Acta Crystallogr*., **B33**, 281–2 (1977).

[33] R. S. Roth and A. D. Wadsley, "Multiple Phase Formation in the Binary System Nb_2O_5–WO_3: III. The Structure of the Tetragonal Phases," *Acta Crystallogr*., **19**, 38–42 (1965).

[34] R. S. Roth and A. D. Wadsley, "Multiple Phase Formation in the Binary System Nb_2O_5–WO_3: IV. The Block Principle," *Acta Crystallogr*., **19**, 42–7 (1965).

[35] R. C. Buchanan, *Materials Crystal Chemistry*. CRC Press, Boca Raton, FL, 1997.

[36] Y. Ni, J. M. Hughes, and A. N. Mariano, "Crystal Chemistry of the Monazite and Xenotime Structures," *Am. Mineral*., **80** [1] 21–6 (1995).

[37] Y. Hikichi, T. Nomura, Y. Tanimura, S. Suzuki, and M. Miyamoto, "Sintering and Properties of Monazite-Type $CePO_4$," *J. Am. Ceram. Soc*., **73** [12] 3594–6 (1990).

[38] Y. Hikichi, T. Ota, K. Dainmon, T. Hattori, and M. Mizuno, "Thermal, Mechanical and Chemical Properties of Sintered Xenotime-Type RPO_4 (R = Y,Er,Yb or Lu)," *J. Am. Ceram. Soc*., **81** [8] 2216–8 (1998).

[39] O. Sudre, J. Cheung, D. Marshall, P. E. D. Morgan, and C. G. Levi, "Thermal Insulation Coatings of $LaPO_4$," *Ceram. Eng. Sci. Proc*., **4**, 367–74 (2001).

[40] F. Goutenoire, O. Isnard, R. Retoux, and P. Lacorre, "Crystal Structure of $La_2Mo_2O_9$, A New Fast Oxide-Ion Conductor," *Chem. Mater*., **12**, 2575–80 (2000).

[41] K. W. Schlichting, N. P. Padture, and P. G. Klemens, "Thermal Conductivity of Dense and Porous Yttria-Stabilized Zirconia," *J. Mater. Sci*., **36**, 3003 (2001).

[42] P. K. Schelling, S. R. Phillpot, and R. W. Grimes, "Optimum Pyrochlore Compositions for Low Thermal Conductivity By Simulation," *Philos. Mag. Lett*., **84**, 127 (2004).

[43] R. D. Shannon, "Revised Effective Ionic Radii and Systematic Studies of Interatomic Distances in Halides and Chalcogenides," *Acta Crystallogr*., **A32**, 751 (1976).

[44] K. Sickafus, "Layered Atom Arrangements in Complex Materials"; LANL report LA-14205, to be published.

[45] J. M. Ziman, *Electrons and Phonons*. Oxford University Press, Oxford, 2001. □